Chapter 2

Materials and Methods

2.0 Introduction

This chapter describes the selection of raw materials used in the experiments and the various analytical techniques used to determine their physicochemical, elemental, and structural properties. It outlines the experimental setup and methods for single-particle studies, kinetic experiments, and gasification experiments. Additionally, the chapter comprehensively discusses the impact of the operational parameters selected for the study.

2.1 Materials

The research used bamboo and petroleum coke as the primary raw materials presented in Fig 2.1. These materials are examined for their potential to be converted into biofuel. Bambusa *tulda* (B. *tulda*) and petcoke are collected from local market near the University and Numaligrah Refinery, Assam respectively as the raw materials.

2.1.1 Fuel samples

Petroleum coke and bamboo are used as fuel samples in this study. Petroleum coke, commonly called petcoke, is a solid residue produced during petroleum refining. This by-product is produced through deep thermal cracking and condensation reactions that occur at high temperatures within petroleum refineries [78]. Petcoke is a carbon-rich waste material known for its high carbon content, high calorific value, and low ash content. It is often used as a substitute for coal in power plants and various manufacturing industries in India, including cement, steel, and textiles. However, because of its higher carbon content, the combustion of petcoke releases more carbon dioxide than coal, along with other pollutants. This significantly contributes to air pollution and greenhouse gas emissions. Additionally, petcoke commonly contains high levels of sulphur, which can further exacerbate air pollution and lead to the formation of acid rain. Despite these environmental concerns, industries continue to

utilize petcoke, which is readily available and more affordable than other alternatives. The low reactivity of petcoke presents challenges for its utilization as a fuel and limits its thermochemical conversion into value-added products. To utilize petcoke more effectively, it needs to be co-fired with a more reactive fuel with high volatile matter content, such as biomass.

Petroleum coke

Bambusa *tulda* (Bamboo plant)

Fig. 2.1 Fuel samples

Bamboo is the most diverse group of fast-growing perennial plants in the *Poaceae* (Gramineae) grass family. It is an important non-wood biomass resource that grows in forests and non-forest areas across India [101, 102]. Bamboos are commonly found in tropical Asian countries such as India, China, Thailand, and Myanmar. According to the India State Forest Report 2021, there are around 125 indigenous and 11 exotic bamboo species in India. More than 50% of these bamboo species grow in Arunachal Pradesh, Assam, Manipur, Nagaland, and West Bengal. The most commonly cultivated bamboo species in Assam are Bambusa *balcooa* (Bhaluka bamboo), Bambusa *tulda* (Jati bamboo), Malocanna *bacciferra* (Muli bamboo), Dendrocala mus*hamiltonii* (Koko bamboo), and Dendrocalamus *giganteus* (Mokalm bamboo) [103].

Bamboo is a promising biomass source for energy generation due to its renewable nature, cost-effectiveness, and carbon neutrality. It sequesters the same amount of carbon during its growth as is emitted when it is used as fuel. Bamboo is the fastest-growing plant, with growth

rates of up to 91 cm per day, leading to high biomass productivity. Unlike non-renewable fossil fuels, bamboo can be replenished over time and does not result in additional carbon emissions during its use. Bamboo has excellent fuel characteristics, including high volatile matter, calorific value, and low ash content. Additionally, its moisture content is significantly lower than that of other biomass types. The lignocellulosic components in bamboo can comprise up to 70 % of its composition, with minimal variation among different species. These properties make bamboo highly relevant for thermochemical conversion processes [104,105]. Thermochemical conversion is an efficient method for generating sustainable energy with significant potential for scaling up. Using bamboo as an energy source can reduce reliance on fossil fuels while contributing to a sustainable energy supply [106, 107]. It is essential to understand its physiochemical properties, thermal degradation behaviour, effects of heating rates, and the chemical reaction mechanisms involved to successfully convert bamboo into value-added biofuel.

2.2. Methods

2.2.1. Sample characterization

The biomass fuel samples were cut into small pieces before sun-drying. After drying, the materials are pulverized and sieved to achieve a uniform particle size of less than 250 micrometers (μm). The processed samples are then stored in an airtight container for further characterization and preparation. The physicochemical properties of the pulverized samples are evaluated through various analytical methods, including proximate analysis and ultimate analysis. Proximate analysis is performed to assess the fuel quality based on fixed carbon, moisture content, volatile matter, and ash content. The fixed carbon content is calculated using the difference indicated in equation 2.1.

$$FC = 100 - MC - VM - Ash \qquad [2.1]$$

Where, FC = fixed carbon, wt %; VM = volatile matter (wt% on dry basis); MC= moisture (wt% on dry basis); Ash = ash (wt% on dry basis). The Mettler Toledo SB24001 Delta Range

balance is used in these combustion experiments and has a maximum weighing capacity of 24,100 grams. For weights up to 4,800 grams, the balance has the accuracy of 0.1 grams; for weights exceeding this limit, the accuracy is 1 gram. This high-resolution capability allows for real-time monitoring of weight changes during combustion, essential for accurately capturing subtle variations in mass loss. The balance features an RS232 interface that enables seamless data logging, enhancing reliability and minimizing manual errors. Additionally, its robust construction and user calibration feature ensures consistent measurements, further ensuring the reliability of the collected data.

The ultimate analysis of all fuel samples is conducted using a CHN analyser (model: PE 2400 series II, PERKIN ELMER, USA) to determine the concentrations of carbon (C), hydrogen (H), and nitrogen (N). The higher heating values (HHV) are measured with a bomb calorimeter (model: 5E-1AC/ML). Composition analysis is performed to assess the lignocellulosic components of biomass, specifically hemicellulose, cellulose, and lignin. In this study, hemicellulose, cellulose, and lignin content are determined following the procedures outlined by Lin *et al.* (2010) [108]. Table 2.1 presents the physicochemical properties of B. *tulda* and petcoke fuel samples. Both B. *tulda* and petcoke exhibit low moisture content, measured at 8.32 % and 1.73 %, respectively, which makes them ideal for combustion. Another crucial factor influencing fuel reactivity is the volatile matter (VM) content. Here, petcoke shows lower reactivity with a VM of 9.87 %, while B. *tulda* has a much higher reactivity with a VM of 72.42 %. Both fuel samples feature low ash content, which reduces the risk of agglomeration or sintering during combustion. The ultimate analysis reveals a significant difference in carbon content between the fuel samples: petcoke has a carbon content of 86.56 %, whereas B. *tulda* has only 45.47 %. Despite this difference, the nitrogen content for both samples is approximately 2 %, indicating low NO_x emissions during combustion. Moreover, the caloric value of petcoke is higher than that of B. *tulda*. The elemental and structural morphology of the samples is analyzed using Scanning Electron Microscopy-Energy Dispersive X-ray

Analysis (SEM-EDX). The SEM JEOL JSM-6390LV is used for analysis. X-ray Diffraction (XRD) is conducted using a BRUKER AXS FOCUS (Model D8 Focus and Mini Flex) with Cu Kα radiation (λ = 1.5406 Å). Fourier Transform Infrared Spectroscopy (FTIR) analysis is carried out to identify the functional groups present in the samples using a Nicolet Model Impact 410 (USA). For this analysis, an alkali halide, KBr powder, is mixed with the sample and then pressed into a pellet, which is examined in the wave number range of 500–4000 cm^{-1}.

Table 2.1 Physicochemical properties of *B. tulda* and petcoke

Samples	**B. *tulda***	**Petcoke**
Proximate analysis (%) (dry basis)		
Moisture content	8.32±1.21	1.70±0.5
Volatile matter	72.42±3.8	9.87±1.2
Ash content	2.41±0.81	0.98±0.2
Fixed carbon	16.85	87.42
Ultimate analysis (%) (dry basis)		
Carbon	45.47±5.1	86.56±6.2
Hydrogen	6.08±1.6	3.51±1.1
Nitrogen	2.0±0.8	2.5±0.6
Oxygen	46.45	7.43
Calorific value (MJ/kg)	17.85±1.4	38.22±3.2

2.2.2. Pyrolysis experiments in TGA

Thermogravimetric analysis

The thermal decomposition study of Bambusa *tulda* (B. *tulda*) is conducted using a thermogravimetric analyzer (Mettler Toledo DTG60). Fig. 2.2 presents the photograph of the thermogravimetric analyzer. Each fuel sample is heated from ambient temperature to 1273 K at heating rates of 10, 20, and 30 K min^{-1} under two different environments: (a) pure nitrogen (N_2) and (b) carbon dioxide (CO_2) at a flow rate of 50 mL min^{-1} in the TGA instrument. The TGA data are recorded to estimate the kinetic parameters. Non-isothermal runs are performed using an initial mass of 12 ± 0.5 mg and a particle size of fewer than 250 micrometers to minimize diffusion effects. Nitrogen is purged through the furnace before each experiment to eliminate the atmospheric air. Similarly, the kinetic study is conducted

using the same TGA instrument under a CO_2 atmosphere, maintaining the same temperature range and heating rates, to examine the effects of blending petcoke with B. *tulda* on the kinetic triplets. The blended fuel samples are designated as follows: B100P0 (100 % B. *tulda* and 0 % petcoke), B80P20 (80 % B. *tulda* and 20 % petcoke), B60P40 (60 % B. tulda and 40 % petcoke), B40P60 (40 % B. *tulda* and 60 % petcoke), and B0P100 (0 % B. *tulda* and 100 % petcoke).

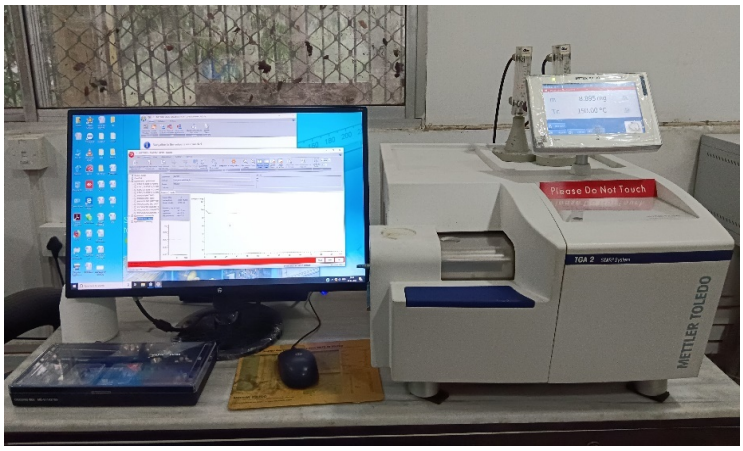

Fig. 2.2 Thermogravimetric analyzer

Devolatilization index

The devolatilization characteristics of B. *tulda* samples are examined to study the effects of four heating rates. The parameters analyzed include the initial temperature (T_i) marks the onset of devolatilization, peak temperature (T_p) corresponds to the maximum point in the temperature profile, after which it begins to decline, maximum weight loss rate ($-R_p$), average weight loss rate ($-R_v$), temperature range at half of weight loss ($-R_p$ ($\Delta T_{1/2}$), and the final thermal degradation temperature (T_f) marks the end of devolatilization, where the profile reaches plateau. The comprehensive devolatilization index (D_i) is calculated using equation 2.2, as provided by Chen *et al.* (2017) [44].

$$D_i = \frac{(-R_p) \times (-R_v)}{T_i \times T_p \times \Delta T_{1/2}} \qquad [2.2]$$

Kinetic study

The pyrolysis behaviour differs among various biomass types due to variations in composition and structure. However, the general process of biomass pyrolysis can be outlined as follows:

$$Biomass = Volatiles + gases + char$$

The data of the thermal conversion process are fitted to a series of model–free methods to study the reaction mechanism. The kinetics of solid-state decomposition are usually based on equation 2.3.

$$\frac{d\alpha}{dt} = k(T)f(\alpha) \qquad [2.3]$$

Where, $\frac{d\alpha}{dt}$ is the isothermal reaction rate, *k(T)* is the reaction rate constant, which is a function of temperature, and $f(\alpha)$ is the reaction model in the differential form. Arrhenius's equation generally represents the reaction rate constant as expressed by equation 2.4.

$$k(T) = A\ exp\left(\frac{E_a}{RT}\right) \qquad [2.4]$$

Where, A is the pre-exponential factor, E_a is the activation energy, R is the universal gas constant (8.314 J K^{-1} mol^{-1}) and T is the absolute temperature. The overall change in the physical property is observed from the thermo-gravimetric analysis data and is determined as the conversion fraction (α). The values of 'α' are evaluated as the fraction of total weight loss in the process, as shown in equation 2.5.

$$\alpha = \frac{W_o - W_t}{W_o - W_f} \qquad [2.5]$$

Where, W_o is the initial weight, W_t is the weight at a given instant of time t, W_f is the final weight of the unreacted solid residues which remain after the reaction [43, 109]. The iso–conversional methods are generally used for the interpretation of processes that are more complex and where many chemical reactions transpire simultaneously. Therefore, their reaction mechanisms are not exactly known. The iso–conversional methods can be either differential or integral to investigate the TGA data [53, 109]. The kinetics of biomass thermal

decomposition is commonly predicted as a single-step reaction and could express itself as the isothermal condition. The reaction rate can also be written by combining the equation 2.3 and 2.4 and expressed by equation 2.6.

$$\frac{d\alpha}{dt} = k(T)f(\alpha) = A\exp\left(\frac{E_a}{RT}\right) f(\alpha) \qquad [2.6]$$

The non–isothermal rate expression, which represents rates of reaction as the function of temperature at linear heating rate (β) can be expressed through superficial transformations as given in equation2.7.

$$\frac{d\alpha}{dT} = \frac{d\alpha}{dt}\frac{dt}{dT} \qquad [2.7]$$

Where, $\frac{dt}{dT}$ is the inverse of heating rate, $\frac{1}{\beta}$, and $\frac{d\alpha}{dt}$ is the non–isothermal reaction rate. An expression for the rate law of the non–isothermal condition can be acquired by substituting equation 2.7 into equation 2.6 and expressed in the equation 2.8.

$$\frac{d\alpha}{dT} = \frac{k(T)}{\beta}f(\alpha) = \left(\frac{A}{\beta}\right)\exp\left(\frac{E_a}{RT}\right) f(\alpha) \qquad [2.8]$$

The integral form of equation 2.8 can be expressed as follows in the equation2.9.

$$g(\alpha) = \int_0^{\alpha} \frac{d\alpha}{f(\alpha)} = \frac{A}{\beta}\int_{T_o}^{T} exp\left(-\frac{E_a}{RT}\right)dT \qquad [2.9]$$

The iso–conversional method can follow either a differential or integral methods to investigate the TGA data.

Friedman method

In this study, the Friedman method is used as a differential iso–conversional technique that can be expressed in general terms as given in equation 2.10 [110].

$$\frac{d\alpha}{dt} = \beta\left(\frac{d\alpha}{dT}\right) = Aexp\left(\frac{-E_a}{RT}\right)f(\alpha) \qquad [2.10]$$

Taking natural logarithms of each side from equation 2.10 yields the equation 2.11.

$$\ln\left(\frac{d\alpha}{dt}\right) = ln\left[\beta\left(\frac{d\alpha}{dT}\right)\right] = ln[Af(\alpha)] - \frac{E_a}{RT} \qquad [2.11]$$

In the above differential iso–conversional method, the reaction model function $f(\alpha)$ is assumed to remain constant. The apparent activation energy (E_a) can be determined by plotting $\ln\left[\beta\left(\frac{d\alpha}{dT}\right)\right]$ versus $\frac{1}{T}$ which yields a straight line, and the slope corresponds to $\left(-\frac{E_a}{R}\right)$ for any constant value of α.

Flynn–Wall–Ozawa (FWO) method

The FWO is an integral iso–conversion technique based on Doyle's equation for approximation of temperature integral and the equation is given in equation 2.12 [38].

$$ln\beta = ln\left(\frac{AE_a}{Rg(\alpha)}\right) - 5.331 - 1.052\frac{E_a}{RT} \qquad [2.12]$$

Where, at a given value of conversion, $g(\alpha)$ is constant and the plot of $ln\beta$ versus $\frac{1}{T}$ represents a linear relation with a given value of conversions. The apparent activation energy (E_a) can be determined coming from the slope ($-1.052\frac{E_a}{R}$).

Kissinger Akahira (KAS) method

The KAS is another extensively used integral iso–conversional method based on the equation 2.13 given below [38].

$$ln\left(\frac{\beta}{T^2}\right) = ln\left(\frac{AR}{E_a g(x)}\right) - \frac{E_a}{RT} \qquad [2.13]$$

For the KAS method, plot $ln\left(\frac{\beta}{T^2}\right)$ versus $\left(\frac{1}{T}\right)$, at the fixed value of conversion at different heating rates from which the E_a can be determined from the slope of the plot.

Evaluation of reaction mechanism and pre–exponential factor

The evaluation of the reaction mechanism and pre–exponential factor through the iso–conversional methods is not straightforward. The method does not allow for a simple evaluation of the kinetic parameters i.e. A and $f(\alpha)$. Hence, among several other parameters that are proposed, the Criado master plot and compensation factors are used to evaluate, plot, and calculate the reaction mechanism and the pre–exponential factors.

Criado master plots

Following the International Confederation of Thermal Analysis and Calorimetry (ICTAC), $Z(\alpha)$ master plots may be applied to determine the reaction model from the exemplar set of models [53]. The master plots are characteristic curve, generally independent of the kinetic parameters like Ea and A but depends on the kinetic model of the process. Criado master plots incorporated by differential and integral forms of reaction model are used to determine the most appropriate kinetic model [111-113]. The generalized equation of Criado master plot is as follows [114].

$$\frac{Z}{Z_{0.5}} = \frac{f(\alpha)g(\alpha)}{f(0.5)g(0.5)} = \left(\frac{T}{T_{0.5}}\right)^2 \times \left[\frac{\theta(d\alpha/d\theta)}{\theta(d\alpha/d\theta)_{0.5}}\right] \qquad [2.14]$$

Where, $T_{0.5}$ and $\left({}^{d\alpha}/_{d\theta}\right)_{0.5}$ are the temperature and rate at the reference point $\alpha = 0.5$. The shape of the theoretical $Z(\alpha)$ master plot can be determined by the given differential, $f(\alpha)$and integral, $g(\alpha)$ forms of kinetic models listed in Table 2.2. The experimental values of $Z(\alpha)/Z(0.5)$ are determined for each value of α by the experimental results of Ea, $d\alpha/dt$ and T_α under different heating rates using three model–free methods (Friedman, FWO, KAS). The resulting experimental values and theoretical master plot of $Z(\alpha)$ are plotted against α and compared to predict the most appropriate kinetic model.

Compensation effect

Although the iso-conversional method provides optimum activation energy, the compensation factor guides accurately determining the pre–exponential factor (A). The Arrhenius parameter can be evaluated by substituting the most appropriate kinetic model predicted by the Criado master plot. A strong correlation in the form of linear relationship between the Arrhenius parameters, lnA_j and Ea_j estimated using single heating rate method, is known as compensation effect.

Table 2.2 Kinetic models of solid–state reactions in differential and integral form

Reaction mechanism		Differential form, $f(\alpha)$	Integral form, $g(\alpha)$
A2	Avrami–Erofeev	$2(1-\alpha)[-\ln(1-\alpha)]^{1/2}$	$[-\ln(1-\alpha)]^{1/2}$
A3	Avrami–Erofeev	$3(1-\alpha)[-\ln(1-\alpha)]^{2/3}$	$[-\ln(1-\alpha)]^{1/3}$
A4	Avrami–Erofeev	$4(1-\alpha)[-\ln(1-\alpha)]^{3/4}$	$[-\ln(1-\alpha)]^{1/4}$
D1	One–Dimensional Diffusion	$1/2\alpha^{-1}$	α^2
D2	Two–Dimensional Diffusion (Valensi Equation)	$[-\ln(1-\alpha)]^{-1}$	$(1-\alpha)\ln(1-\alpha)+\alpha$
D3	Three–Dimensional Diffusion (Jander Equation)	$3/2(1-\alpha)^{2/3}[1-(1-\alpha)^{1/3}]^{-1}$	$[1-(1-\alpha)^{1/3}]^2$
D4	Three–Dimensional Diffusion (Ginstling–Brounshtein Equation)	$3/2[1-(1-\alpha)^{1/3}]^{-1}$	$[1-(2/3)\alpha]-(1-\alpha)^{2/3}$
F1	First–Order Reaction	$1-\alpha$	$-\ln(1-\alpha)$
F2	Second–Order Reaction	$(1-\alpha)^2$	$(1-\alpha)^{-1}-1$
P2	Power Law	$2\alpha^{1/2}$	$\alpha^{1/2}$
P3	Power Law	$3\alpha^{2/3}$	$\alpha^{1/3}$
P4	Power Law	$4\alpha^{3/4}$	$\alpha^{1/4}$
R2	Contracting Area	$2(1-\alpha)^{1/2}$	$[1-(1-\alpha)]^{1/2}$
R3	Contracting Volume	$3(1-\alpha)^{2/3}$	$[1-(1-\alpha)]^{1/3}$

Taking natural logarithmic of equation 2.8, we can get the equation 2.15.

$$ln\left(\frac{(d\alpha/dt)}{f_i(\alpha)}\right) = lnA_i(\alpha) - \frac{Ea(\alpha)}{RT} \qquad [2.15]$$

Where, i indicate the reaction models predicted by the master plots. Selecting the predicted kinetic model and by plotting the left-hand side of the equation 2.15 to the inverse of temperature, $(1/T)$, a pair of lnA_i and Ea_i can be generated from the intercept and slope of the straight line. The compensation factor equation is given as follows:

$$lnA_i = a^* Ea_i + b^* \qquad [2.16]$$

Where, $a^*$and b^*, can be generated from the linear fitting of the pair $ln\,A_i$ and E_{a_i}. Once the values of $a^*$and b^* parameters are obtained, the pre–exponential factor; $ln\,A_\alpha$ can be determined by using the equation 2.16.

$$lnA_\alpha = a^* Ea + b^* \qquad [2.17]$$

The E_a values used in equation 2.17 are obtained with iso-conversional methods which lead to the model–free values of A_α. The kinetic analysis of biomass pyrolysis typically involves studying the mechanisms and rates of the chemical reactions that take place during the conversion of biomass. Hence, conducting kinetic study before thermal conversion is critical as it can provide valuable information about the reaction rates and other factors that can influence the process efficiency. This understanding can be effectively used in regulating reactions in industrial operations, contributing significantly to accurate process design, product yield management, and improved reactor design, while optimizing its operational parameters [47].

2.2.3 Pyrolysis in a fixed bed system

A fixed-bed pyrolysis reactor is used for the pyrolysis experiments of B. *tulda*, as outlined in the schematic diagram of the pyrolysis system (Fig. 2.3). A series of biomass pyrolysis experiments are conducted using a vertical fixed-bed pyrolysis reactor made of stainless steel, which measured 75 cm in length, with an internal diameter of 2 cm and a wall thickness of 0.23 cm. The reactor is heated by radiant heaters and insulated with quartz wool. Thermocouples are used to monitor the temperatures within the pyrolysis reactor and to regulate the radiant heaters throughout the experiment. Computer-controlled valves managed the gas flow within the reactor. Each experiment involved loading 8 g of the B. *tulda* sample into the fixed-bed pyrolysis reactor. Before starting the experiment, nitrogen (N_2) is purged for 10 minutes to ensure an inert atmosphere inside the reactor. The heater controller is programmed to gradually increase the temperature from room temperature to 973 K at atmospheric pressure, with a heating rate of 10 K per minute. During the pyrolysis experiment, pure gas is introduced at a mass flow rate of 15 ml per minute. The same parameters are maintained for pyrolysis conducted under CO_2 atmosphere. Once the reactor reached the desired temperature, it is maintained for 30 minutes. Afterwards, the gas flow and heater controller are deactivated, allowing the reactor to cool to ambient temperature before collecting the char samples. The char samples from B. *tulda* are then stored in a

desiccator for further characterization. The char produced from B. *tulda* under nitrogen atmosphere is labelled as BCN, while the char produced under carbon dioxide atmosphere is labelled as BCC.

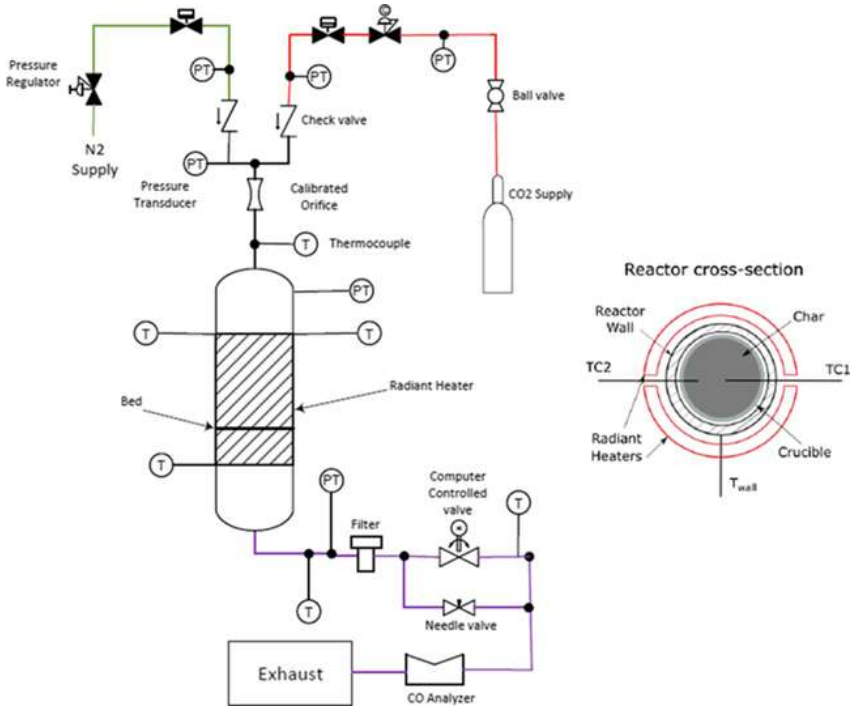

Fig. 2.3 Schematic diagram of tubular fixed-bed reactor arrangement and instrumentation [82]

Energy balance

This investigation aimed to determine the weight difference and energy output during the pyrolysis of B.*tulda* char under nitrogen and carbon dioxide atmospheres. The mass yield, higher heating value of the samples on dry basis, and energy yield of the char are calculated based on the equations 2.18-2.20 [115].

$$Mass\ yield\ (\%) = \left(\frac{mass\ of\ bamboo\ char}{mass\ of\ raw\ bamboo}\right) \times 100 \qquad [2.18]$$

$$HHV_{daf}\left(\frac{MJ}{kg}\right) = \left(\frac{HHV\ of\ sample}{1 - fraction\ of\ dry\ ash\ insample}\right) \qquad [2.19]$$

$$Energy\ yield\ (\%) = (mass\ yield) \times \left(\frac{HHV_{daf}\ of\ bamboo\ char}{HHV_{daf}\ of\ raw\ bamboo}\right) \qquad [2.20]$$

Characterization of bamboo char

The physicochemical properties of BCN and BCC, generated under nitrogen and carbon dioxide atmospheres, are analysed using the same techniques employed for the B. *tulda* samples. The elemental and structural morphology of the char samples are examined using Scanning Electron Microscopy with Energy Dispersive X-ray Analysis (SEM-EDX). The SEM analysis is conducted with a JEOL JSM-6390LV instrument. For X-ray Diffraction (XRD) analysis, a BRUKER AXS FOCUS system (Model D8 Focus and Miniflex) is used, utilizing Cu Kα radiation with a wavelength of λ = 1.5406 Å. Fourier Transform Infrared Spectroscopy (FTIR) analysis is performed to identify the functional groups present in the samples using a Nicolet Impact 410 spectrometer. In this procedure, an alkali halide, potassium bromide (KBr) powder, is mixed with the sample and pressed into a pellet for analysis in the 500–4000 cm^{-1} wave number range.

2.2.4. Single-particle combustion

This study conducted a single-particle combustion experiment to investigate mass degradation and the duration of combustion stages. The experiment helps compare and validate the thermal degradation behaviour predicted in the kinetic study. Pulverized B. *tulda* and petcoke are blended in various mass ratios for single-particle combustion. The two materials are mixed at different blend ratios and formed into spherical shapes with diameters of 20 mm, 25 mm, and 30 mm, using water as a binder (see Fig. 2.4). The moulding process is performed manually, applying consistent hand pressure to ensure adequate compaction and binding for each sample. After moulding, the samples are allowed to air dry before being placed in an oven for further drying. The blended fuel samples, which varied in blend ratios and diameters, are dried in a hot air oven at 378 K for 8 hours, followed by an additional 8 hours of air drying to ensure uniform moisture content. The samples are visually inspected for shape consistency and structural stability, checking for any signs of cracking to confirm uniformity. Table 2.3 presents the proportions of the fuel samples used for blending and the designated names assigned to each sample. The experiments are conducted in a controlled

laboratory environment without windows to minimize external influences. Fuel samples were ignited externally using a firing lamp. Ceiling fans are turned off during the experiments to maintain uniform air distribution in the room and ensure the stability of the combustion flame. Each experiment is repeated three times to verify the reliability and consistency of the results. The standard deviation method is used to report the average values, which provides a measure of the variability in the experimental data. This approach enhances the accuracy of the findings by quantifying the degree of variation and offering a more reliable representation of the experimental results.

Table 2.3 Sample names and B. *tulda*/petcoke blend percentages of fuel samples

Sample name	Blend ratio		Volatile matter (%)	Particle density (kg/m^3)
	B. *tulda* (%)	Petcoke (%)		
B100P0	100	0	72.42	462.0±7.5
B90P10	90	10	67.74	541.5±8.2
B80P20	80	20	62.50	586.1±7.2
B70P30	70	30	56.23	666.4±7.8
B60P40	60	40	44.69	707.3±9.3

The markers for '*flame extinction*' and '*complete burnout*' during combustion are identified through visual observations of the fuel samples and their mass degradation behavior. Flame extinction occurs when the visible flame diminishes and the sample ceased to emit a bright luminous glow, indicating the end of volatile combustion. Complete burnout is recognized when mass degradation reaches a plateau, indicating that the char has been fully consumed, with no further visible combustion activity or significant mass loss. This method relies on visual observation but has consistently shown reliable results across repeated experiments. It is supported by the mass degradation profile, which ensures accurate identification of the combustion stages. A Nikon camera (D5600) is used to capture the behavior of flame. The camera has a resolution of 24.2 mega pixels and a maximum aperture of f/5.6, with a shutter speed that ranges from 1/4000 of a second to 30 seconds. The resolution of the camera is 1920 x 1080 pixels.

Spherical fuel samples, which vary in blend ratios and diameters, are used in a single-particle combustion experiment conducted in an air atmosphere. Fig. 2.4 presents the photographs of pulverized B.*tulda* and petcoke and blended fuel samples. The fuel sample is suspended from a laboratory tripod using a wire mesh to ensure consistent exposure to air and flame during combustion. This setup is placed on an electronic balance to monitor weight loss throughout the combustion process, with mass degradation recorded at 30-second intervals (see Fig. 2.5).

B. *tulda* Petcoke Blended samples

Fig. 2.4 Photographs of pulverized B.*tulda* and petcoke and blended fuel samples

Fig. 2.5 Experimental set up of combustion experiments

The combustion process is primarily divided into two stages: (a) volatile burning time (also known as flaming time), which indicates the duration between the onset and offset of the volatile flame, and (b) char combustion time (referred to as glowing time), which represents the period from the extinguishing of the flame to the final burnout of the char [62]. After burning the fuel samples, the remaining ash is collected in a steel pan to investigate how

blending impacts its composition. The ash is then analysed using Energy Dispersive X-ray (EDX) and X-ray Diffraction (XRD) techniques to determine its crystalline properties and elemental composition. Additionally, the ignition mass flux was determined using measured parameters like density, flaming time, and surface area-to-volume ratio (SA/V). The ignition mass flux was calculated by dividing the density of the fuel by the product of flaming time and SA/V [65]. The research examines how varying blend ratios of B. *tulda* and petcoke affect flame characteristics, ignition temperature, burnout rate, and ash residue. Combining biomass with petcoke has the potential to enhance thermal efficiency and support sustainable co-combustion systems.

2.2.5. CO_2 gasification experiment

A fixed-bed downdraft gasification system is used for the CO_2 gasification experiment. Fig. 2.6 shows the schematic representation of the system. The gasifier consists of a 76 cm long stainless steel tubular reactor with a diameter of 2 cm and a wall thickness of 0.23 cm. A stainless-steel crucible holds the samples inside the reactor, supported by a rod connected to a mesh. Two radiant heaters are used to heat a 30 cm section of the reactor, and the setup is insulated with quartz wool to minimize heat loss. The temperature is monitored and controlled by K-type thermocouples and a PID controller for the radiant heater. Nitrogen (N_2) and carbon dioxide (CO_2) gases are used during the heating and gasification, and the supply is regulated by a computerized valve. It allowed for pressure control by regulating the mass flow of gas while maintaining the desired temperature and volume. Six pressure transducers monitored the pressure, and a calibrated orifice maintained the consistent mass flow rate during the gasification process. The carbon monoxide (CO) concentration in the downstream syngas generation is measured using a HORIBA Mexa 311GE CO analyzer. A LabVIEW virtual instrument is also used to acquire and record signals from the pressure transducers, thermocouples, and control valves.

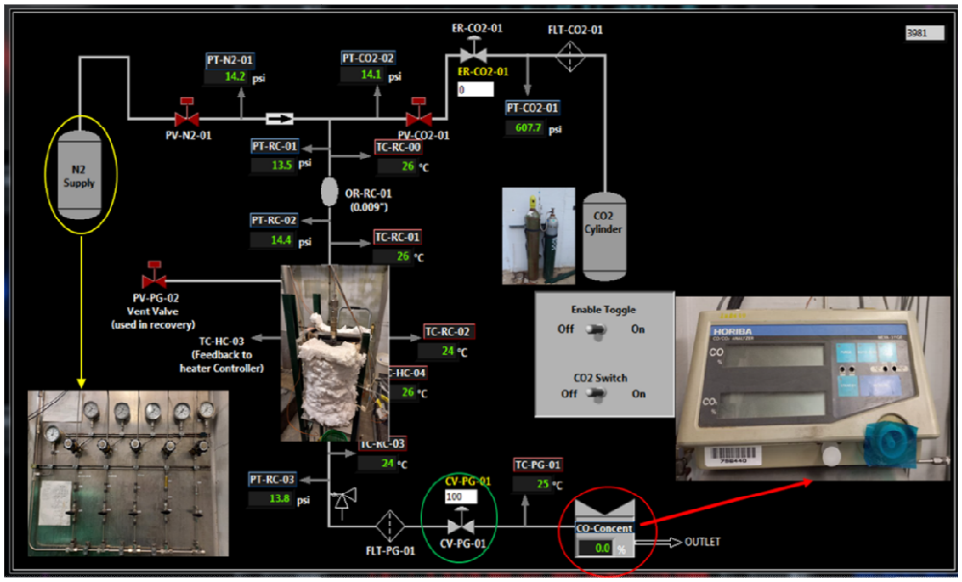

Fig. 2.6 Schematic of the gasification system with experimental setup photos, including the gasifier reactor**,** N_2 and CO_2 supplies, and Horiba gas analyser

Sample preparation process and pyrolysis

The wet impregnation technique is used to impregnate bamboo samples with a potassium carbonate (K_2CO_3) catalyst. Initially, 0.36 g of K_2CO_3 is dissolved in 250 ml of deionized water and stirred for 24 hours using a magnetic stirrer to make an aqueous solution of the catalyst. Subsequently, 16 g of pulverized bamboo (with a particle size of less than 150 µm) is added to the solution, stirring for 24 hours to ensure homogeneous catalyst loading. Finally, the mixture is dried for 48 hours at 378 K. The pyrolysis experiments on the impregnated bamboo samples are conducted in a tubular fixed-bed reactor under inert conditions after the catalyst impregnation. Nitrogen gas (N_2) is used for pyrolysis at a flow rate of 0.25 g/s. The reactor temperature is increased from ambient conditions to 973 K at a rate of 30 K per minute, and a residence time of 30 minutes is maintained to ensure the effective removal of moisture and volatile matter from the samples. The resulting bamboo char is analysed using Field Emission Scanning Electron Microscopy (FESEM) and Energy Dispersive X-ray Spectroscopy (EDX) to assess its surface morphology and determine the elemental composition with and without the catalyst loading. After the pyrolysis process, one portion of

the K_2CO_3-impregnated bamboo char is used for a CO_2 gasification experiment to investigate the effects of operational parameters. Another portion of the K_2CO_3-impregnated bamboo char is blended with petcoke to study the synergistic effects of blending during the CO_2 gasification experiment. The blending ratios tested are 100% bamboo char and 0% petcoke (B100P0), 80% bamboo char and 20% petcoke (B80P20), 60% bamboo char and 40% petcoke (B60P40), and 50% bamboo char and 50% petcoke (B50P50) respectively.

CO_2 gasification process

A fuel sample weighing 0.3 g is used in the reactor for the gasification experiment. The sample is heated from room temperature to the desired temperature using a constant flow of nitrogen (N_2) at a rate of 0.25 g/s to prevent premature oxidation and remove moisture from the fuel sample. The pressure inside the reactor is controlled by a computerized control valve once the desired temperature is reached. The nitrogen flow is replaced with carbon dioxide using a National Instruments virtual instrument to initiate the gasification reaction. The mole fraction of carbon monoxide (CO) in the syngas is continuously monitored throughout the experiment. The experiment is conducted for 60 minutes under different temperatures (1023 K, 1123 K, and 1173 K) and pressures (1 atm, 3 atm, and 5 atm), within the hardware limits. The gasification process is considered complete when the CO mole fractions curve stabilized, showing no significant fluctuations. Finally, the ash residue is collected for further study of the char conversion and properties.

Measurements of char conversion

The char conversion calculation over time uses a global heterogeneous reaction, as presented by equation 2.21. The gasification reaction of char with carbon dioxide is represented by the overall C-CO_2 reaction [116]. Carbon monoxide (CO) concentration is measured in the synthesis gas, along with the mass flow rates, to quantify the apparent char conversion rates over time. Based on the mass conservation principle, CO and char production rates are related, as shown in equation 2.22.

$$C\ (char) + CO_2 = 2CO \qquad \Delta H = 172\ Kg\ mol^{-1} \qquad [2.21]$$

$$\dot{\omega}_{CO} = y_{CO}\dot{m}_{out} = -2\dot{\omega}_{char}\frac{MW_{CO}}{MW_{char}} \qquad [2.22]$$

Where, $\dot{\omega}_{CO}$ is the mass production rate of CO, y_{CO} is the mole fraction of CO in the product mixture, $\dot{m}_{out}$ is the total mass flow rate of the outgoing gases. MW_{CO} is the molecular weight of CO and MW_{char} is the molecular weight of char. The changes in char mass over time and char conversion are determined by measuring CO concentration, as described in equation 2.23. The final char conversions are assessed by weighing the post-gasification feedstock with a micro-balance scale. These results are compared to the final conversion calculated from gas composition analysis (equation 2.24).

$$m_{char,t} = m_{char,t=0} - \frac{MW_{char}}{2MW_{CO}}\int_0^t \dot{\omega}_{CO}\,dt \qquad [2.23]$$

$$X = 1 - \frac{m_{char,t}}{m_{char,t=0}} \qquad [2.24]$$

The initial mass of char is denoted as $m_{char,t} = 0$, while the mass of char at time t is represented as $m_{char,t}$. The final char conversions are determined by measuring the mass of the feedstock after gasification using a micro-balance scale. The measurements are then compared to the final conversions obtained from gas composition analysis.

2.3 Summary

This chapter presents the materials used in the current study. It includes detailed information on the methods used to characterize and analyse the feedstock. Additionally, a thorough description of the experimental setup for combustion, pyrolysis (utilizing both thermogravimetric analysis and a fixed-bed system), and the gasification process is provided. Furthermore, the chapter discusses the methods, measurements, and data analysis techniques used to achieve the objectives of this research.